

# 1 Glycolytic reprogramming underlies immune cell activation by polyethylene wear 2 particles

3  
4 Chima V. Maduka<sup>1,2,3</sup>, Oluwatosin M. Habeeb<sup>2,3</sup>, Maxwell M. Kuhnert<sup>2,3</sup>, Maxwell  
5 Hakun<sup>2,3</sup>, Stuart B. Goodman<sup>4,5</sup>, Christopher H. Contag<sup>2,3,6\*</sup>

6  
7 <sup>1</sup> Comparative Medicine & Integrative Biology, Michigan State University, East Lansing, MI 48824, USA

8 <sup>2</sup> Department of Biomedical Engineering, Michigan State University, East Lansing, MI 48824, USA

9 <sup>3</sup> Institute for Quantitative Health Science & Engineering, Michigan State University, East Lansing, MI  
10 48824, USA

11 <sup>4</sup> Department of Orthopedic Surgery, Stanford University, CA 94063, USA.

12 <sup>5</sup> Department of Bioengineering, Stanford University, CA 94305, USA.

13 <sup>6</sup> Department of Microbiology & Molecular Genetics, Michigan State University, East Lansing, MI 48864,  
14 USA.

15

16 \*Christopher H. Contag, [contagch@msu.edu](mailto:contagch@msu.edu)

17

## 18 Abstract

19 Primary total joint arthroplasties (TJAs) are widely and successfully applied reconstructive  
20 procedures to treat end-stage arthritis. Nearly 50% of TJAs are now performed in young  
21 patients, posing a new challenge: performing TJAs which last a lifetime. The urgency is  
22 justified because subsequent TJAs are costlier and fraught with higher complication rates,  
23 not to mention the toll taken on patients and their families. Polyethylene particles,  
24 generated by wear at joint articulations, drive aseptic loosening by inciting insidious  
25 inflammation associated with surrounding bone loss. Down modulating polyethylene  
26 particle-induced inflammation enhances integration of implants to bone  
27 (osseointegration), preventing loosening. A promising immunomodulation strategy could  
28 leverage immune cell metabolism, however, the role of immunometabolism in  
29 polyethylene particle-induced inflammation is unknown. Our findings reveal that immune  
30 cells exposed to sterile or contaminated polyethylene particles show fundamentally  
31 altered metabolism, resulting in glycolytic reprogramming. Inhibiting glycolysis controlled  
32 inflammation, inducing a pro-regenerative phenotype that could enhance  
33 osseointegration.

34

35 **Keywords:** Polyethylene wear particles, glycolytic reprogramming, total joint  
36 arthroplasty, immune cells

37

## 38 Introduction

39 End-stage arthritis can be successfully treated by primary total joint arthroplasties  
40 (TJAs)<sup>1</sup>. With nearly 50% of TJAs performed in patients younger than 65 years<sup>2</sup>, the vision  
41 of TJAs is now to reconstruct joints which will last a lifetime, despite patients' daily  
42 activities<sup>3</sup>. This is especially crucial because revision TJAs are costlier and fraught with  
43 higher complication rates, technical difficulties, and poorer surgical outcomes than  
44 primary TJAs<sup>4</sup>. Such revision TJAs commonly arise from aseptic loosening, frequently  
45 incited by polyethylene wear particles generated by relative motion at joint articulations<sup>5</sup>.  
46 Aseptic loosening may occur with or without adsorbed contaminants, such as bacterial

47 lipopolysaccharides (LPS). Wear particles induce prolonged, low-grade inflammation with  
48 macrophages and fibroblasts as key immune cellular players<sup>6</sup>. This pathology is often  
49 radiographically detected only when surrounding bone loss (periprosthetic osteolysis)  
50 occurs<sup>3</sup>. By then, compromised implant stability results in loosening and implant failure,  
51 necessitating revision surgeries.

52 To minimize generation of wear particles, ultrahigh molecular weight polyethylene  
53 liners at the bearing surfaces of reconstructed joints are currently being replaced by highly  
54 crosslinked polyethylene. Crosslinked polyethylene has significantly reduced the amount  
55 of generated wear particles and accompanied chronic inflammation with periprosthetic  
56 osteolysis<sup>7</sup>. However, crosslinking does not completely block the generation of wear  
57 particles from bearing surfaces of implants and subsequent inflammation<sup>8</sup>. Up to 9% of  
58 patients with crosslinked polyethylene liners present with chronic inflammation-induced  
59 periprosthetic osteolysis 15 years later<sup>9</sup>. Moreover, crosslinking has little effect on  
60 particles from third body wear, backside wear and impingement<sup>10</sup>; and there are currently  
61 no agents that specifically treat polyethylene particle-induced inflammatory osteolysis<sup>11</sup>.  
62 Consequently, there is an unmet clinical need to develop methods that will mitigate  
63 aseptic loosening from polyethylene particle-induced chronic inflammation to improve  
64 implant longevity. Furthermore, as particles generated from ultrahigh molecular weight or  
65 highly crosslinked polyethylene similarly result in inflammation<sup>8,11</sup>, either of them  
66 effectively models particle-induced inflammation.

67  
68  
69

70 Metabolic reprogramming refers to changes in glycolytic flux and oxidative  
71 phosphorylation (OXPHOS), traditional bioenergetic pathways, that are inextricably linked  
72 to macrophage activation toward proinflammatory<sup>12,13</sup> or pro-regenerative  
73 phenotypes<sup>14,15</sup>. Advances in understanding macrophage-mesenchymal stem cell  
74 crosstalk<sup>16</sup> has revealed that down modulating inflammation induced by polyethylene  
75 particles can prevent implant loosening by enhancing osseointegration through increased  
76 pro-regenerative macrophage activity. For example, using mesenchymal stem cells  
77 (MSCs)<sup>17</sup> and engineered IL-4 expressing MSCs<sup>18</sup>; targeting inflammatory pathways  
78 using decoy molecules for NF- $\kappa$ B<sup>19</sup>, TNF- $\alpha$ <sup>20</sup> and MCP-1<sup>21</sup>; and using antioxidants like  
79 vitamin E<sup>11</sup> have shown promise for enhanced osseointegration by reducing  
80 inflammation. However, the metabolic underpinnings underlying macrophage activation  
81 by polyethylene particles are largely undefined. A detailed understanding of metabolic  
82 programs could be leveraged for immunomodulation toward extending the longevity of  
83 implants. Here, we show that both macrophages and fibroblasts exposed to sterile or  
84 LPS-contaminated polyethylene particles undergo metabolic reprogramming and  
85 differential changes in bioenergetics. Glycolytic reprogramming underlies increased  
86 levels of proinflammatory cytokines, including MCP-1, IL-6, IL-1 $\beta$  and TNF- $\alpha$ . Specific  
87 inhibition of different glycolytic steps not only modulated these proinflammatory cytokines  
88 but stimulated pro-regenerative cytokines, including IL-4 and IL-10, without affecting cell  
89 viability. Concomitant elevation of both glycolytic flux and oxidative phosphorylation by  
90 polyethylene particles and inhibitory effects on inflammatory cytokines in addition to IL-

91  $1\beta^{13}$  suggest a unique metabolic program that could be targeted for pro-regenerative  
 92 clinical outcomes following TJAs.

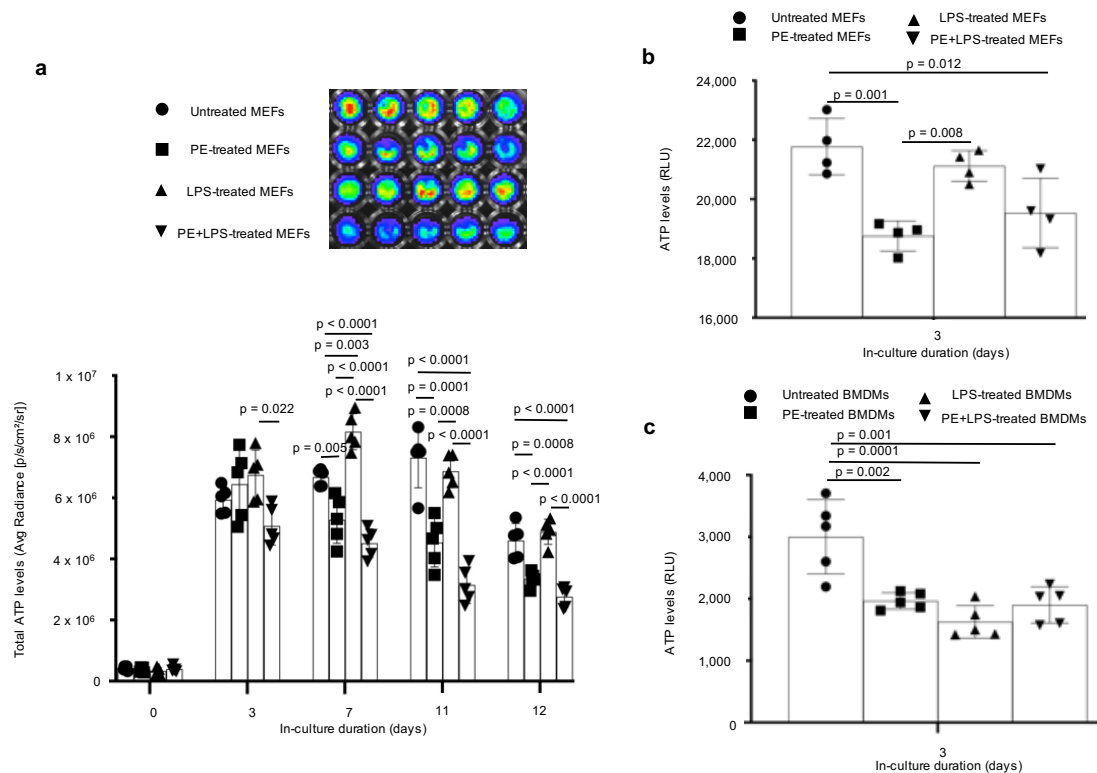


**Figure 1 | Ultrahigh molecular weight polyethylene (PE) particles, alone or in combination with endotoxin (LPS), alter bioenergetic (ATP) levels. a.** Over time, PE particles lower bioenergetics in blasticidin-eGFP-luciferase (BGL)-transfected mouse embryonic fibroblasts (MEFs) compared to untreated cells; combining PE particles and LPS lowers ATP levels compared to PE particles or LPS alone (representative bioluminescent wells shown). **b.** In lysed wild-type MEFs, bioenergetics is lowered after exposure to PE particles. **c.** In primary bone marrow-derived macrophages (BMDMs), PE particles and LPS, alone or in combination, decrease bioenergetics. Mean (SD), n = 5 (Fig. 1a, 1c), n = 4 (Fig. 1b), one-way ANOVA followed by Tukey's post-hoc test.

93  
 94 **Results**  
 95 **Bioenergetics is differentially altered in immune cells exposed to polyethylene**  
 96 **particles**

97 We had previously optimized an in-vitro, live-cell, bioenergetic workflow where  
 98 ATP is rate-limiting to measure spatiotemporal bioenergetic alterations in cells exposed  
 99 to biomaterials<sup>22</sup>. This involved transfecting mouse embryonic fibroblasts (MEFs) with a  
 100 Sleeping Beauty transposon plasmid (pLuBIG) having a bidirectional promoter driving an  
 101 improved firefly luciferase gene (fLuc) and a fusion gene encoding a Blasticidin-resistance  
 102 marker (BsdR) linked to eGFP (BGL)<sup>23</sup>. Both highly crosslinked<sup>8</sup> and ultrahigh molecular  
 103 weight<sup>21</sup> polyethylene particles similarly incite inflammation and are clinically used.  
 104 Ultrahigh molecular weight polyethylene particles whose doses and sizes have been  
 105 previously characterized were examined herein after polyethylene particles were  
 106 determined to be endotoxin-free<sup>17-19,21</sup>. Since adsorbed bacterial lipopolysaccharide (LPS;  
 107 a.k.a. endotoxin) could play a role in aseptic loosening<sup>24</sup>, we compared key results to cells  
 108 exposed to polyethylene particles and LPS.

109 Whereas only polyethylene particles consistently lowered bioenergetic (ATP)  
110 levels in live BGL cells, overall, LPS alone did not affect ATP levels when compared to  
111 untreated fibroblasts over time (Fig. 1a). In comparison to polyethylene particles or LPS  
112 alone, combining polyethylene particles and LPS further decreased ATP levels after  
113 prolonged exposure (Fig. 1a). D-luciferin used in live-cell assays could be limited by its  
114 ability to permeate cell membranes<sup>25</sup>; accordingly, bioenergetic measurement in lysed  
115 fibroblasts was more sensitive, corroborating decreases in ATP levels after exposure to  
116 only polyethylene particles (by 1.2-fold) or a combination of polyethylene particles and  
117 LPS (by 1.1-fold) relative to untreated cells at day 3 (Fig. 1b). Primary bone marrow-  
118 derived macrophages revealed a 1.5-, 1.8-, and 1.6-fold decrease in ATP levels relative  
119 to untreated cells following exposure to only polyethylene particles, only LPS, and  
120 polyethylene particles with LPS, respectively (Fig. 1c).

### 121 122 **Exposure to polyethylene particles alters functional metabolism in immune cells**

123 To explore what bioenergetic pathways were responsible for alterations in ATP  
124 levels, we used the Seahorse assay to probe extracellular acidification rate (ECAR),  
125 lactate-linked proton efflux rate (PER) and oxygen consumption rate (OCR). ECAR, PER  
126 and OCR are indices of glycolytic flux, monocarboxylate transporter (MCT) function<sup>26,27</sup>  
127 and mitochondrial oxidative phosphorylation, respectively, and are used to assess  
128 metabolic reprogramming<sup>12,13</sup>. Following exposure to LPS alone, fibroblasts did not reveal  
129 changes in ECAR, PER or OCR compared to untreated cells (Fig. 2a-c). In contrast,  
130 exposure to polyethylene particles resulted in a 1.7-, 1.7-, and 2-fold increase in ECAR,  
131 PER and OCR, respectively, relative to untreated fibroblasts (Fig. 2a-c). Similarly, a  
132 combination of polyethylene particles and LPS increased OCR by 1.6-fold in comparison  
133 to untreated fibroblasts (Fig. 2c).

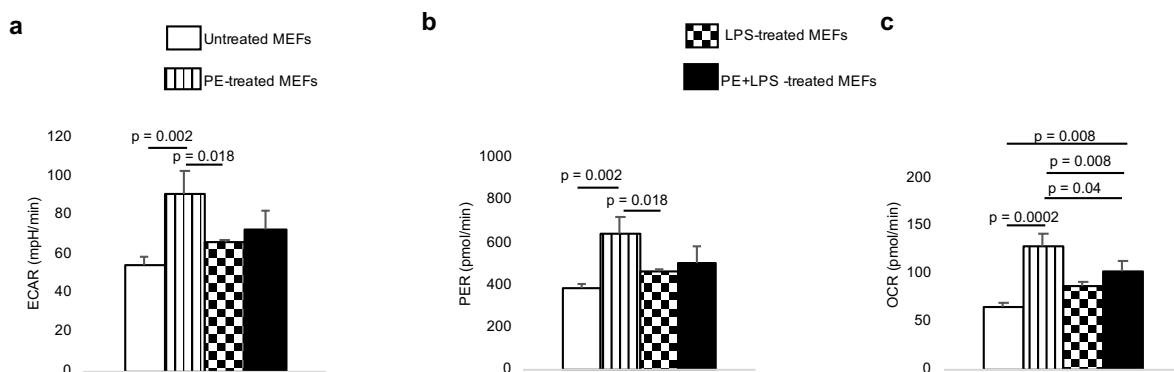


**Figure 2 | Mouse embryonic fibroblasts (MEFs) exposed to ultrahigh molecular weight polyethylene (PE) particles alone show increased functional metabolic indices.** a-c, In comparison to untreated cells, PE particle-treated MEFs have higher extracellular acidification rate (ECAR; a), proton efflux rate (PER; b) and oxygen consumption rate (OCR; c). Mean (SD), n = 3, one-way ANOVA followed by Tukey's post-hoc test.

134  
135 Exposure to only polyethylene particles increased ECAR, PER and OCR by 13.1-  
136 , 13.1- and 3.1-fold, respectively, in primary macrophages compared to untreated cells  
137 (Fig. 3a, c, e). Macrophages exposed to polyethylene particles and LPS increased ECAR,

138 PER and OCR by 23-, 23.1- and 2.8-fold, respectively, compared to untreated cells (Fig.  
139 3b, d, f).

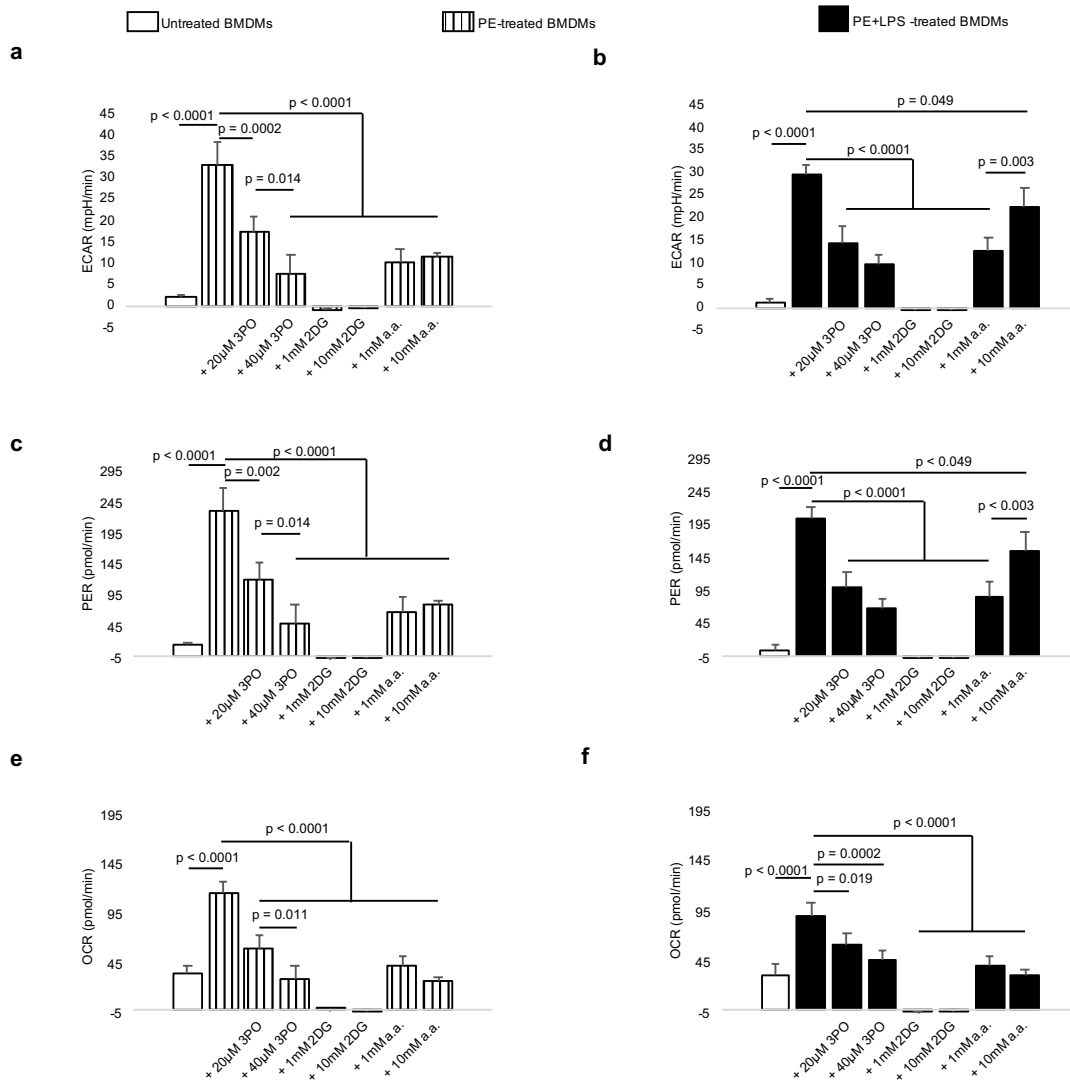


**Figure 3 | Primary bone marrow-derived macrophages (BMDMs) exposed to ultrahigh molecular weight polyethylene (PE) particles or both PE particles and endotoxin (LPS) reveal greater extracellular acidification rate (ECAR), proton efflux rate (PER) and oxygen consumption rate (OCR) than untreated cells; this increment is reduced upon addition of various glycolytic inhibitors. a-f, ECAR (a-b), PER (c-d) and OCR (e-f) are increased in BMDMs treated with PE particles, alone or in combination with LPS; elevated levels are decreased upon addition of 3-(3-Pyridinyl)-1-(4-pyridinyl)-2-propen-1-one (3PO), 2-deoxyglucose (2DG) or aminoxyacetic acid (a.a.). Mean (SD), n = 3, one-way ANOVA followed by Tukey's post-hoc test.**

140

141 To reduce abnormal increments in ECAR, PER and OCR, we targeted different  
142 stages of glycolysis using 3-(3-pyridinyl)-1-(4-pyridinyl)-2-propen-1-one (3PO), 2-  
143 deoxyglucose (2DG) and aminoxyacetic acid (a.a.). 3PO inhibits 6- phosphofructo-2-  
144 kinase which is the rate limiting glycolytic enzyme<sup>28</sup>; 2DG inhibits hexokinase, the first  
145 enzyme in glycolysis<sup>13</sup>; and a.a. prevents the mitochondrion from utilizing glycolytic  
146 pyruvate<sup>29</sup>. In a dose-dependent manner, 3PO, 2DG and a.a. decreased ECAR, PER and  
147 OCR among macrophages exposed to only polyethylene particles or a combination of

148 polyethylene particles and LPS (Fig. 3a-f), suggesting efficient cellular uptake and  
 149 pharmacologic effects of these small molecule inhibitors.

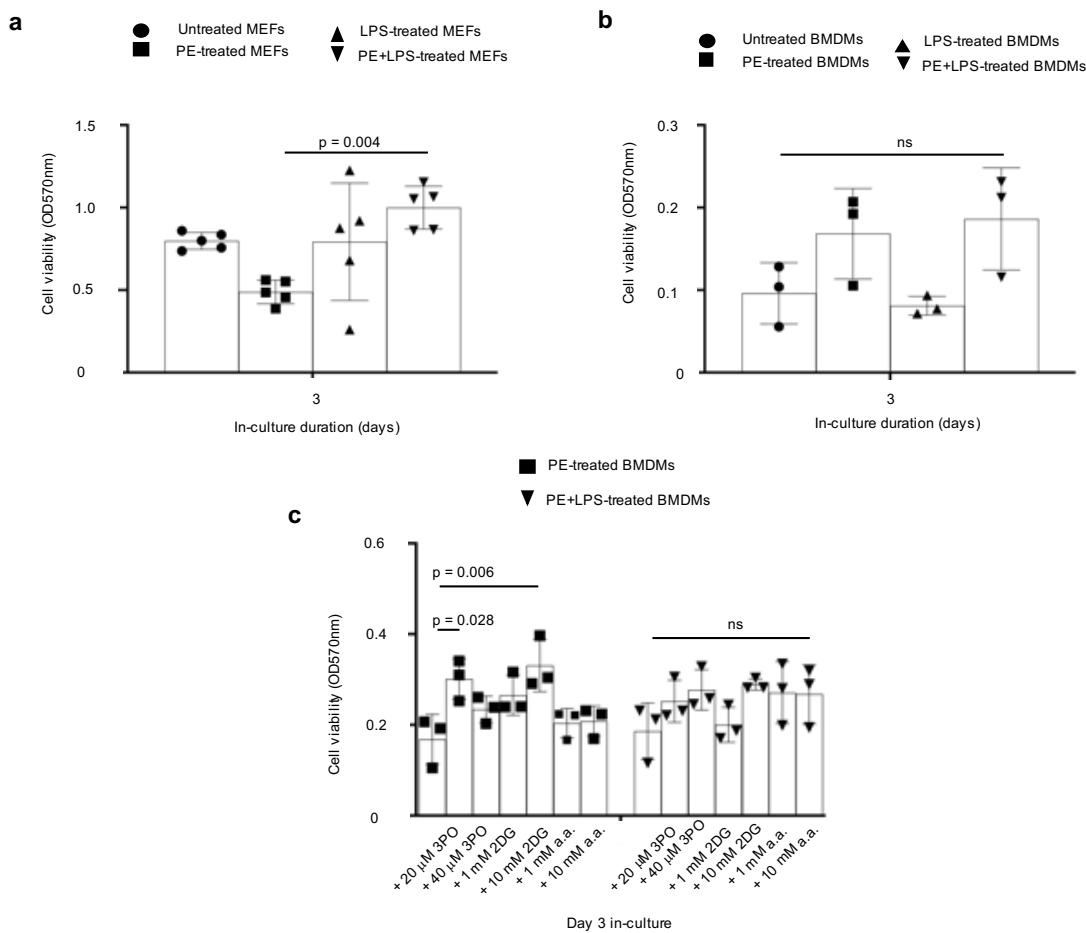


**Figure 4 | Compared to untreated cells, treatment with ultrahigh molecular weight polyethylene (PE) particles, endotoxin (LPS) or a combination of PE particles and LPS does not change cell numbers; addition of glycolytic inhibitors does not decrease cell numbers. a-b.** In mouse embryonic fibroblasts (MEFs; a) or primary bone marrow-derived macrophages (BMDMs; b), exposure to PE particles, LPS or PE particles and LPS does not change cell numbers relative to untreated controls. **c.** Addition of various doses of 3-(3-Pyridinyl)-1-(4-pyridinyl)-2-propen-1-one (3PO), 2-deoxyglucose (2DG) or aminooxyacetic acid (a.a.) to PE particle-treated or PE particle- and LPS-treated BMDMs does not decrease cell numbers. Mean (SD), n = 5 (Fig. 4a), n = 3 (Fig. 4b, c), one-way ANOVA followed by Tukey's post-hoc test.

150

151 Compared to untreated cells, there was no difference in cell numbers following  
 152 exposure to polyethylene particles, LPS or polyethylene particles with LPS among  
 153 fibroblasts (Fig. 4a) or macrophages (Fig. 4b). Additionally, exposure of macrophages to  
 154 pharmacologic inhibitors, including 3PO, 2DG and a.a. did not lower cell viability (Fig. 4c).  
 155 Importantly, in fibroblasts exposed to polyethylene particles alone or polyethylene  
 156 particles and LPS, addition of 3PO, 2DG or a.a. further lowered bioenergetics in a dose-  
 157 dependent manner (Fig. 5).

158

### 159 Immunometabolism underlies macrophage polarization by polyethylene particles

160

161 To evaluate how metabolism affects immune cellular function, we assayed levels  
 162 of cytokine and chemokine expression using a magnetic bead-based technique<sup>30</sup>. We  
 observed that proinflammatory proteins, including MCP-1 (Fig. 6a), IL-6 (Fig. 6b), IL-1β



163 (Fig. 6c) and TNF- $\alpha$  (Fig. 6d) were increased by 4.1-, 97.3-, 41.8- and 7-fold, respectively,  
 164 after exposure to polyethylene particles in comparison to untreated macrophages.

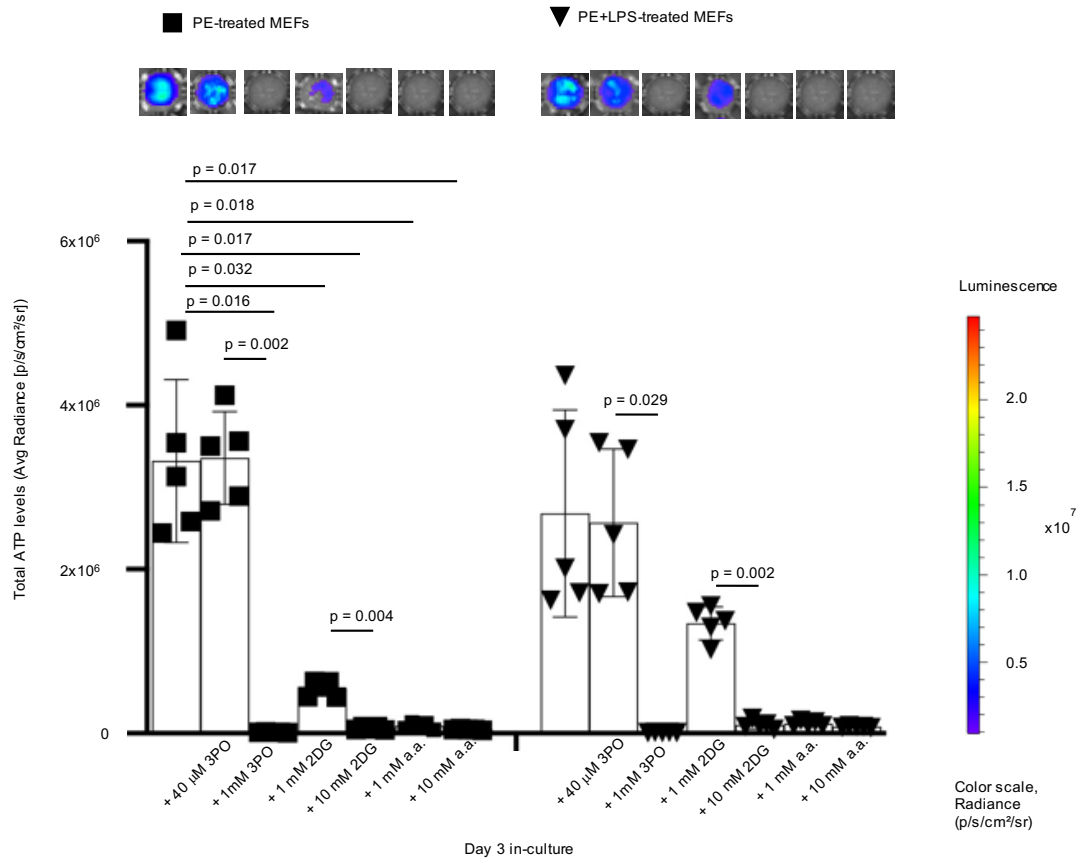


**Figure 5 | Glycolytic inhibitors decrease bioenergetic levels in treated mouse embryonic fibroblasts (MEFs).** Following treatment of blasticidin-GFP-Luciferase (BGL)-transfected MEFs with ultrahigh molecular weight polyethylene (PE) particles alone or in combination with endotoxin (LPS), addition of 3-(3-pyridinyl)-1-(4-pyridinyl)-2-propen-1-one (3PO), 2-deoxyglucose (2DG) and aminooxyacetic acid (a.a.; representative wells are shown) tend to decrease bioenergetics in a dose-dependent manner. Not significant (ns), mean (SD), Brown-Forsythe and Welch ANOVA followed by Dunnett's T3 multiple comparisons test, n = 5.

165  
 166 Addition of 3PO or 2DG consistently decreased proinflammatory cytokine or  
 167 chemokine levels (Fig. 6a-d) relative to macrophages exposed to only polyethylene  
 168 particles; however, addition of a.a. selectively decreased MCP-1 expression (Fig. 6a).  
 169 Exposure of macrophages to polyethylene particles decreased IL-4 levels by 7.4-fold  
 170 compared to untreated cells; addition of 3PO, 2DG or a.a. increased IL-4 levels by 2.9-  
 171 4.3-, and 1.5- fold, respectively, relative to polyethylene particles alone; however, only the  
 172 increase by 2DG was statistically significant (Fig. 6e). Levels of IL-13 and IFN- $\lambda$  were  
 173 unchanged (data not shown). Consistent with macrophage polarization being a  
 174 continuum<sup>31,32</sup>, polyethylene particles increased IL-10 expression in comparison to  
 175 untreated macrophages (Fig. 6f). Whereas addition of 3PO or 2DG did not increase IL-  
 176 10 levels, a.a. increased IL-10 expression by 3.2-fold relative to macrophages exposed  
 177 to only polyethylene particles (Fig. 6f).

178  
 179

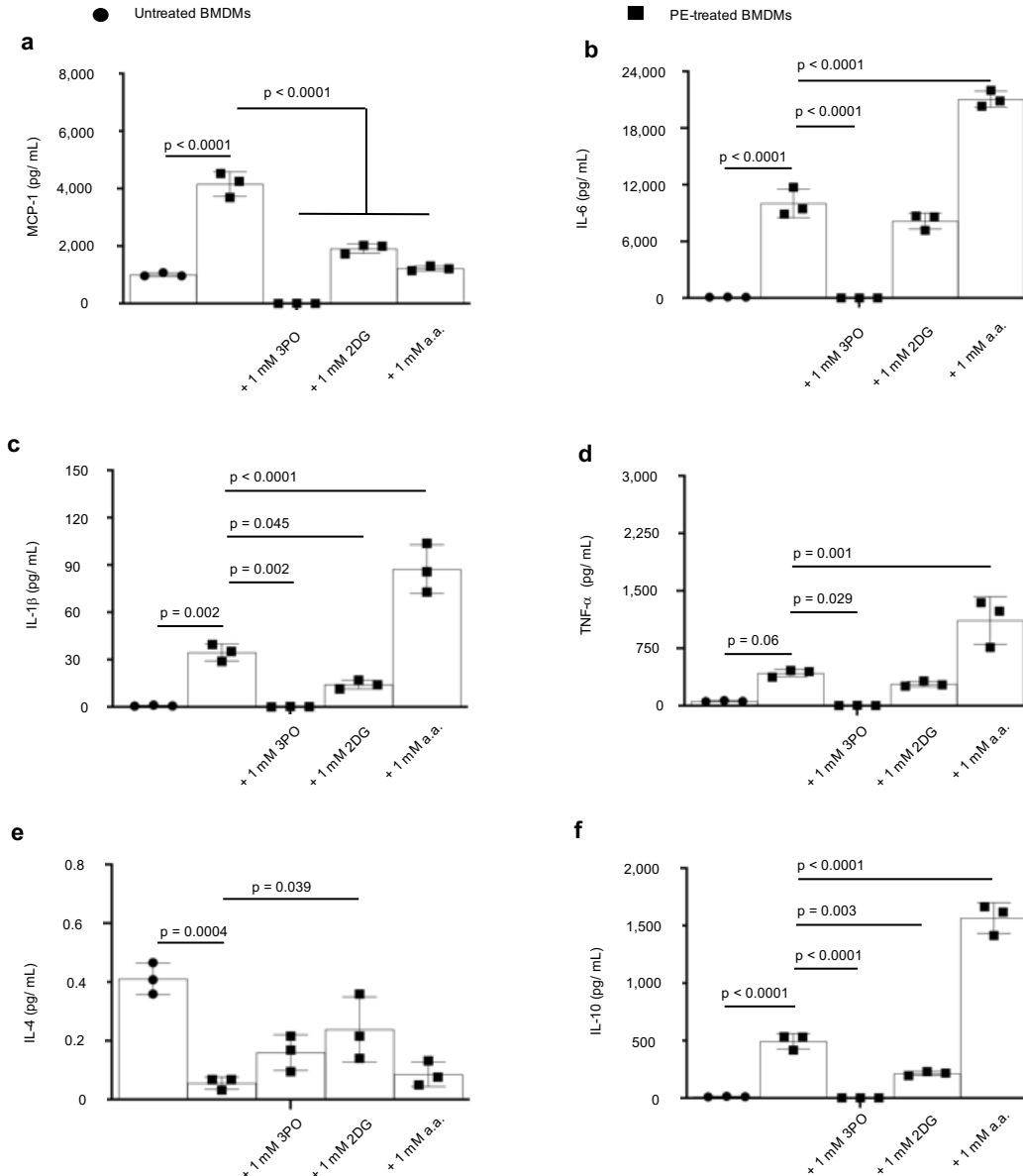


**Figure 6 | Elevated proinflammatory cytokine (protein) levels are decreased following addition of glycolytic inhibitors to primary bone marrow-derived macrophages (BMDMs).** a-d, In BMDMs, exposure to ultrahigh molecular weight polyethylene (PE) particles increase proinflammatory cytokines, including MCP-1 (a), IL-6 (b), IL-1 $\beta$  (c) and TNF- $\alpha$  (d) in comparison to untreated BMDMs. Addition of 3-(3-Pyridinyl)-1-(4-pyridinyl)-2-propen-1-one (3PO) or 2-deoxyglucose (2DG) decreases proinflammatory cytokines; aminoxyacetic acid (a.a.) selectively decreases MCP-1 levels. e, Exposure of BMDMs to PE particles decreases IL-4 levels in comparison to untreated cells; IL-4 levels tend to increase following addition of glycolytic inhibitors. f, Compared to BMDMs exposed to only PE particles, exposure to PE particles and a.a. increase IL-10 levels. Mean (SD), n = 3, one-way ANOVA followed by Tukey's post-hoc test; assay was performed after 3 days in-culture.

## 180 Discussion

181 When macrophages are exposed to bacterial lipopolysaccharide (LPS), their  
 182 bioenergetic (ATP) levels are decreased as part of cell activation and inflammation<sup>33</sup>. This  
 183 results from reprogrammed metabolism that shifts bioenergetic dependence from  
 184 mitochondrial oxidative phosphorylation (OXPHOS) to glycolysis, with crucial  
 185 consequences on proinflammatory<sup>12,13</sup> and anti-inflammatory<sup>14,15</sup> events. While  
 186 immunometabolism in response to LPS has been well characterized for such clinical  
 187 applications as bacterial sepsis, the role of immunometabolism in sterile inflammation  
 188 induced by clinically relevant implant materials is unknown.



189 Macrophages are the dominant immune cell type implicated in the chronic  
190 inflammatory response to ultrahigh molecular weight polyethylene (PE) particles<sup>2</sup>, likely  
191 acting through Toll-like receptors (TLRs)<sup>34,35</sup>. Following exposure to PE particles of  
192 particular sizes and over a threshold, transcriptional signaling occurs through NF- $\kappa$ B<sup>36</sup>,  
193 MyD88<sup>37</sup> and chemerin/ChemR23<sup>38</sup>. Consequently, there is increased production of  
194 proinflammatory cytokines that accompany resulting pathologies, including periprosthetic  
195 osteolysis. Likewise, fibroblasts play a synergistic role with macrophages. Fibroblasts  
196 exposed to PE particles<sup>39,40</sup> express MCP-1, RANKL, IL-1 $\beta$ , IL-6, MMP1 and MMP2  
197 which activate osteoclasts, accentuate inflammation and degrade surrounding bone  
198 extracellular matrix.

199 Adsorbed LPS could be a contaminant on sterilized implants and has been  
200 documented in a subset of patients diagnosed with aseptic loosening of implants from  
201 chronic inflammation<sup>24</sup>, and could exacerbate PE particle-induced inflammation<sup>41</sup>.  
202 Therefore, PE and LPS-contaminated PE (cPE) particles were examined and compared  
203 to LPS. Our findings reveal that bioenergetic imbalances differentially occur in  
204 macrophages and fibroblasts exposed to PE particles, LPS or cPE particles. For example,  
205 although LPS did not affect ATP levels in fibroblasts, PE particles lowered cellular  
206 bioenergetics. Furthermore, fibroblasts exposed to PE particles but not LPS were  
207 metabolically reprogrammed, revealing increases in glycolysis, OXPHOS and  
208 monocarboxylate transporter (MCT) function. On the other hand, decreased ATP levels  
209 were observed in primary bone marrow-derived macrophages exposed to PE particles,  
210 LPS or cPE particles consistent with reliance on glycolysis. Immune cells depend on  
211 glycolysis during inflammatory activation as glycolysis produces ATP quicker than  
212 OXPHOS, albeit OXPHOS results in overall higher ATP levels. Additionally, this switch to  
213 glycolysis is crucial for IL-1 $\beta$  production by stabilizing HIF-1 $\alpha$  in macrophages<sup>13</sup> and  
214 fibroblast activation in fibrosis<sup>42</sup>. Surprisingly, in addition to elevated glycolysis, OXPHOS  
215 was increased in macrophages exposed to PE or cPE particles, independent of changing  
216 cell numbers. Concomitant elevation in both glycolysis and OXPHOS suggests a unique  
217 metabolic reprogram induced by PE particles relative to LPS; LPS increases glycolysis  
218 while reducing OXPHOS<sup>12</sup>. Accompanied decrease in ATP levels suggests that increased  
219 OXPHOS is directed at functions other than cellular energy supply. In a septic model,  
220 LPS was shown to repurpose mitochondrial function toward superoxide formation in  
221 macrophages<sup>12</sup>. At earlier time points than used in this study, LPS decreased OXPHOS<sup>12</sup>,  
222 likely reflecting as yet uncharacterized temporal changes in metabolic reprogramming.  
223 Notably, glycolytic flux and MCT function but not OXPHOS were higher in macrophages  
224 exposed to cPE than PE particles, relative to respective controls. This may likely be from  
225 synergistic signaling with cPE particles, as PE particles and LPS are known to activate  
226 TLR2 and TLR4 receptors, respectively<sup>34,35</sup>.

227 Elevated glycolytic flux in macrophages exposed to PE or cPE particles could be  
228 lowered by specific pharmacologic inhibition of different glycolytic steps using 3-(3-  
229 pyridinyl)-1-(4-pyridinyl)-2-propen-1-one (3PO)<sup>28</sup>, 2-deoxyglucose (2DG)<sup>13</sup> and  
230 aminooxyacetic acid (a.a.)<sup>29</sup>. Lactate from glycolysis is converted to pyruvate which feeds  
231 mitochondrial OXPHOS, and proton-linked lactate is bidirectionally shuttled through  
232 MCT<sup>26,27</sup>. Consequently, pharmacologic inhibition of glycolysis lowered aberrantly

233 elevated OXPHOS and MCT function. Pharmacologic inhibition did not result in reduced  
234 cell viability, excluding potential toxicity. Using fibroblasts expressing luciferase, we  
235 observed that glycolytic inhibition further reduced ATP levels following exposure to PE  
236 particles, corroborating cellular bioenergetic dependence on glycolysis.

237 Contrasting non-degradable PE, polylactide (PLA) is a biodegradable biomaterial.  
238 Degradation products of PLA, oligomers and monomers of lactic acid, increase ATP  
239 levels only after prolonged exposure to immune cells, modeling in-vivo conditions<sup>22</sup>.  
240 Increased ATP levels are the result of elevated flux in both glycolysis and mitochondrial  
241 respiration, in-vitro. Corroborating in-vitro observations, radiolabeled glucose uptake was  
242 elevated in a subcutaneous model and shown to drive inflammation to sterile PLA;  
243 targeting glycolysis in-vivo decreased inflammatory markers, including CD86, by reducing  
244 radiolabeled glucose uptake. Similarly, in patients who have undergone total joint  
245 arthroplasties, chronic inflammation by PE particles is often diagnosed by increased  
246 glycolytic flux. Glycolytic flux is measured using fluorodeoxyglucose in positron emission  
247 tomography (PET) combined with computed tomography (CT) or magnetic resonance  
248 imaging (MRI)<sup>43-46</sup>. Our findings suggests that PET imaging is enabled by glycolytic  
249 reprogramming of immune cells in inflamed joints, following exposure to PE or cPE  
250 particles.

251 Macrophages exposed to PE particles became polarized to a proinflammatory  
252 phenotype as measured by elevated protein expression of MCP-1, IL-6, IL-1 $\beta$  and TNF- $\alpha$ .  
253 Additionally, IL-10 was increased, consistent with macrophage polarization being a  
254 spectrum<sup>31</sup>. Both IL-1 $\beta$  and TNF- $\alpha$  induce RANKL expression which drives osteoclast  
255 maturation and differentiation, together with M-CSF<sup>6</sup>. Osteolysis, associated with PE  
256 particle-induced chronic inflammation, is the result of net bone loss from osteoclast-  
257 mediated bone resorption exceeding osteoblast-mediated bone formation. Similarly, IL-  
258 6<sup>47</sup> and MCP-1<sup>48</sup> are associated with increased osteolysis and cartilage destruction.  
259 Interestingly, 2DG and 3PO decreased aberrantly elevated proinflammatory cytokines. In  
260 particular, 2DG allowed for some level of proinflammatory cytokine expression. This is  
261 clinically important because a suitable level of inflammation is required for tissue repair  
262 and osseointegration<sup>49</sup>; compromised osseointegration is a leading cause of implant  
263 failure<sup>4</sup>. Remarkably, whereas 2DG decreased MCP-1, IL-6, IL-1 $\beta$  and TNF- $\alpha$  protein  
264 levels which were elevated by PE particles, 2DG is known to selectively decrease IL-1 $\beta$   
265 protein levels from LPS<sup>13</sup>, suggesting unique differences. In contrast to 2DG and 3PO,  
266 a.a. selectively decreased MCP-1 but not IL-6, IL-1 $\beta$  and TNF- $\alpha$ ; and increased IL-10  
267 levels. Central to macrophage-stem cell crosstalk, IL-10 signaling is critical for tissue  
268 regeneration<sup>50</sup>. Glycolytic inhibition using 2DG increased IL-4 levels which were reduced  
269 by PE particles. Increment of IL-4 levels suggest a pro-regenerative macrophage  
270 phenotype. Acute and chronic inflammation as well as bone loss induced by PE particles  
271 is reversed by inducing a pro-regenerative macrophage phenotype using IL-4<sup>18</sup>.

272 In conclusion, all clinically relevant biomaterials undergo wear at articulations,  
273 resulting in different levels of chronic inflammation and undermining the longevity of  
274 biomaterials used in arthroplasties. By characterizing immune cell metabolism as being  
275 pivotal in the inflammatory pathology induced by polyethylene particles, we reveal a  
276 unique vulnerability which could be harnessed for the dual purposes of controlling

277 inflammation and stimulating pro-regenerative immune cell phenotypes. Targeting  
278 immunometabolism can be extended to other implant materials<sup>51,52</sup>, improving  
279 osseointegration and long-term clinical outcomes for patients undergoing various  
280 arthroplasties.

281

## 282 **Methods**

283 **Materials.** Ultrahigh molecular weight polyethylene particles were sourced, characterized  
284 and determined to be endotoxin-free as previously described<sup>18</sup>. Concentrations of 100ng/  
285 mL of lipopolysaccharide (LPS) from *Escherichia coli* O111:B4 (MilliporeSigma) and 1.25  
286 mg/ mL of ultrahigh molecular weight polyethylene particles were used. Furthermore, 3-  
287 (3-pyridinyl)-1-(4-pyridinyl)-2-propen-1-one (MilliporeSigma), 2-deoxyglucose  
288 (MilliporeSigma) and aminooxyacetic acid (Sigma-Aldrich) were used for glycolytic  
289 inhibition.

290

291 **Bioenergetic measurement.** Bioluminescence was measured using the IVIS Spectrum  
292 in vivo imaging system (PerkinElmer) after adding 150 µg/mL of D-luciferin (PerkinElmer).  
293 Living Image (Version 4.5.2, PerkinElmer) was used for acquiring bioluminescence on the  
294 IVIS Spectrum. Standard ATP/ADP kits (Sigma-Aldrich) containing D-luciferin, luciferase  
295 and cell lysis buffer were used to according to manufacturer's instructions. Luminescence  
296 at integration time of 1,000 ms was obtained using the SpectraMax M3  
297 Spectrophotometer (Molecular Devices) using SoftMax Pro (Version 7.0.2, Molecular  
298 Devices).

299

300 **Cells.** Mouse embryonic fibroblast (MEFs) cell line (NIH 3T3 cell line; ATCC) and primary  
301 bone-marrow derived macrophages (BMDMs) derived from C57BL/6J mice (Jackson  
302 Laboratories) of 3-4 months<sup>12,53</sup> were used. NIH 3T3 cells were stably transfected with a  
303 Sleeping Beauty transposon plasmid (pLuBIG) having a bidirectional promoter driving an  
304 improved firefly luciferase gene (fLuc) and a fusion gene encoding a Blastocidin-resistance  
305 marker (BsdR) linked to eGFP (BGL)<sup>23</sup>. This enabled us to monitor bioenergetic changes  
306 in live cells<sup>22</sup>. For temporal (IVIS) experiments lasting 12 days, 5,000 BGL cells were  
307 initially seeded in each well of a 96-well tissue culture plate in 200 µL of complete medium  
308 (see below). For ATP, crystal violet and Seahorse assays, 20,000 wild-type MEFs were  
309 seeded. For ATP, crystal violet and cytokine/ chemokine assays, 50,000 BMDMs were  
310 seeded; 60,000 BMDMs were seeded for Seahorse experiments. For IVIS experiments  
311 with glycolytic inhibitors, 20,000 BGL cells were initially seeded. All time points are  
312 indicated on respective graphs. Complete medium comprised of DMEM medium, 10%  
313 heat-inactivated Fetal Bovine Serum and 100 U/mL penicillin-streptomycin (all from  
314 ThermoFisher Scientific).

315

316 **Cell viability.** Cell viability was assessed using the crystal violet assay<sup>54</sup>. Absorbance  
317 (optical density) was acquired at 570 nm using the the SpectraMax M3  
318 Spectrophotometer (Molecular Devices) and SoftMax Pro software (Version 7.0.2,  
319 Molecular Devices).

320

321 **Functional metabolism.** Basal measurements of oxygen consumption rate (OCR),  
322 extracellular acidification rate (ECAR) and lactate-linked proton efflux rate (PER) were  
323 obtained in real-time using the Seahorse XFe-96 Extracellular Flux Analyzer (Agilent  
324 Technologies)<sup>12,13,15</sup>. Prior to running the assay, cell culture medium was replaced by the  
325 Seahorse XF DMEM medium (pH 7.4) supplemented with 25 mM D-glucose and 4 mM  
326 Glutamine. The Seahorse ATP rate assay was run according to manufacturer's instruction  
327 and all reagents for the Seahorse assays were sourced from Agilent Technologies. Wave  
328 software (Version 2.6.1) was used to export Seahorse data directly as means  $\pm$  standard  
329 deviation (SD).

330

331 **Chemokine and cytokine measurements.** Cytokine and chemokine levels were  
332 measured using a MILLIPLEX MAP mouse magnetic bead multiplex kit (MilliporeSigma)<sup>30</sup>  
333 to assess for IL-6, MCP-1, TNF- $\alpha$ , IL-1 $\beta$ , IL-4, IL-10, IFN- $\lambda$  and IL-13 protein expression  
334 in supernatants. Data was acquired using Luminex 200 (Luminex Corporation) by the  
335 xPONENT software (Version 3.1, Luminex Corporation). Using the glycolytic inhibitor,  
336 3PO, expectedly decreased cytokine values to  $< 3.2$  pg/ mL in some experiments. For  
337 statistical analyses, those values were expressed as 3.1 pg/ mL. Values exceeding the  
338 dynamic range of the assay, in accordance with manufacturer's instruction, were  
339 excluded. Additionally, IL-6 ELISA kits (RayBiotech) for supernatants were used  
340 according to manufacturer's instructions.

341

342 **Statistics and reproducibility.** Statistical software (GraphPad Prism) was used to  
343 analyse data presented as mean with standard deviation (SD). Significance level was  
344 set at  $p < 0.05$ , and details of statistical tests and sample sizes, which are biological  
345 replicates, are provided in figure legends. Exported data (mean, SD) from Wave in  
346 Seahorse experiments had the underlying assumption of normality and similar variance,  
347 and thus were tested using corresponding parametric tests as indicated in figure  
348 legends.

349

350

## 351 **References**

- 352 1 Ingham, E. & Fisher, J. Biological reactions to wear debris in total joint replacement.  
353 *Proceedings of the Institution of Mechanical Engineers, Part H: Journal of Engineering in*  
354 *Medicine* **214**, 21-37 (2000).
- 355 2 Cobelli, N., Scharf, B., Crisi, G. M., Hardin, J. & Santambrogio, L. Mediators of the  
356 inflammatory response to joint replacement devices. *Nature Reviews Rheumatology* **7**,  
357 600-608 (2011).
- 358 3 Sivananthan, S., Goodman, S. & Burke, M. in *Joint Replacement Technology* 373-402  
359 (Elsevier, 2021).
- 360 4 Goodman, S. B., Gallo, J., Gibon, E. & Takagi, M. Diagnosis and management of implant  
361 debris-associated inflammation. *Expert review of medical devices* **17**, 41-56 (2020).
- 362 5 Bistolfi, A. *et al.* Ultra-high molecular weight polyethylene (UHMWPE) for hip and knee  
363 arthroplasty: The present and the future. *Journal of Orthopaedics* **25**, 98-106 (2021).

- 364 6 Kandahari, A. M. *et al.* A review of UHMWPE wear-induced osteolysis: the role for early  
365 detection of the immune response. *Bone research* **4**, 1-13 (2016).
- 366 7 Tsukamoto, M., Mori, T., Ohnishi, H., Uchida, S. & Sakai, A. Highly cross-linked  
367 polyethylene reduces osteolysis incidence and wear-related reoperation rate in  
368 cementless total hip arthroplasty compared with conventional polyethylene at a mean  
369 12-year follow-up. *The Journal of Arthroplasty* **32**, 3771-3776 (2017).
- 370 8 Ormsby, R. T. *et al.* Osteocytes respond to particles of clinically-relevant conventional  
371 and cross-linked polyethylene and metal alloys by up-regulation of resorptive and  
372 inflammatory pathways. *Acta biomaterialia* **87**, 296-306 (2019).
- 373 9 Hopper Jr, R. H., Ho, H., Sritulanondha, S., Williams, A. C. & Engh Jr, C. A. Otto Aufranc  
374 Award: crosslinking reduces THA wear, osteolysis, and revision rates at 15-year followup  
375 compared with noncrosslinked polyethylene. *Clinical orthopaedics and related research*  
376 **476**, 279 (2018).
- 377 10 Greenfield, E. M. *et al.* Does endotoxin contribute to aseptic loosening of orthopedic  
378 implants? *Journal of Biomedical Materials Research Part B: Applied Biomaterials: An*  
379 *Official Journal of The Society for Biomaterials, The Japanese Society for Biomaterials,*  
380 *and The Australian Society for Biomaterials and the Korean Society for Biomaterials* **72**,  
381 179-185 (2005).
- 382 11 Liu, F., Dong, J., Zhou, D. & Zhang, Q. Identification of key candidate genes related to  
383 inflammatory osteolysis associated with vitamin E-Blended UHMWPE debris of  
384 orthopedic implants by integrated bioinformatics analysis and experimental  
385 confirmation. *Journal of Inflammation Research* **14**, 3537 (2021).
- 386 12 Mills, E. L. *et al.* Succinate Dehydrogenase Supports Metabolic Repurposing of  
387 Mitochondria to Drive Inflammatory Macrophages. *Cell* **167**, 457-470.e413,  
388 doi:10.1016/j.cell.2016.08.064 (2016).
- 389 13 Tannahill, G. *et al.* Succinate is a danger signal that induces IL-1 $\beta$  via HIF-1 $\alpha$ . *Nature* **496**,  
390 238-242, doi:10.1038/nature11986 (2013).
- 391 14 Mills, E. L. *et al.* Itaconate is an anti-inflammatory metabolite that activates Nrf2 via  
392 alkylation of KEAP1. *Nature* **556**, 113 (2018).
- 393 15 Ip, W. E., Hoshi, N., Shouval, D. S., Snapper, S. & Medzhitov, R. Anti-inflammatory effect  
394 of IL-10 mediated by metabolic reprogramming of macrophages. *Science* **356**, 513-519  
395 (2017).
- 396 16 Pajarinen, J. *et al.* Mesenchymal stem cell-macrophage crosstalk and bone healing.  
397 *Biomaterials* **196**, 80-89 (2019).
- 398 17 Lin, T. *et al.* Preconditioning of murine mesenchymal stem cells synergistically enhanced  
399 immunomodulation and osteogenesis. *Stem cell research & therapy* **8**, 1-9 (2017).
- 400 18 Pajarinen, J. *et al.* Interleukin-4 repairs wear particle induced osteolysis by modulating  
401 macrophage polarization and bone turnover. *Journal of Biomedical Materials Research*  
402 *Part A* **109**, 1512-1520 (2021).
- 403 19 Lin, T.-H. *et al.* NF- $\kappa$ B decoy oligodeoxynucleotide enhanced osteogenesis in  
404 mesenchymal stem cells exposed to polyethylene particle. *Tissue engineering Part A* **21**,  
405 875-883 (2015).
- 406 20 Zhao, Y.-p. *et al.* Progranulin suppresses titanium particle induced inflammatory  
407 osteolysis by targeting TNF $\alpha$  signaling. *Scientific reports* **6**, 1-13 (2016).



- 408 21 Gibon, E. *et al.* Selective inhibition of the MCP-1-CCR2 ligand-receptor axis decreases  
409 systemic trafficking of macrophages in the presence of UHMWPE particles. *Journal of*  
410 *Orthopaedic Research* **30**, 547-553 (2012).
- 411 22 Maduka, C. V. *et al.* Polylactide Degradation Activates Immune Cells by Metabolic  
412 Reprogramming. *bioRxiv* (2022).
- 413 23 Kanada, M. *et al.* Differential fates of biomolecules delivered to target cells via  
414 extracellular vesicles. *Proceedings of the National Academy of Sciences* **112**, E1433-  
415 E1442 (2015).
- 416 24 Bonsignore, L. A., Anderson, J. R., Lee, Z., Goldberg, V. M. & Greenfield, E. M. Adherent  
417 lipopolysaccharide inhibits the osseointegration of orthopedic implants by impairing  
418 osteoblast differentiation. *Bone* **52**, 93-101 (2013).
- 419 25 Lee, K. *et al.* Cell uptake and tissue distribution of radioiodine labelled D-luciferin:  
420 implications for luciferase based gene imaging. *Nuclear medicine communications* **24**,  
421 1003-1009 (2003).
- 422 26 Tan, Z. *et al.* in *The Journal of biological chemistry* Vol. 290 46-55 (2015).
- 423 27 Payen, V. L., Mina, E., Van Hee, V. F., Porporato, P. E. & Sonveaux, P. Monocarboxylate  
424 transporters in cancer. *Mol Metab* **33**, 48-66, doi:10.1016/j.molmet.2019.07.006 (2020).
- 425 28 Clem, B. *et al.* Small-molecule inhibition of 6-phosphofructo-2-kinase activity suppresses  
426 glycolytic flux and tumor growth. *Molecular cancer therapeutics* **7**, 110-120 (2008).
- 427 29 Kauppinen, R. A., Sihra, T. S. & Nicholls, D. G. Aminooxyacetic acid inhibits the malate-  
428 aspartate shuttle in isolated nerve terminals and prevents the mitochondria from  
429 utilizing glycolytic substrates. *Biochim Biophys Acta* **930**, 173-178, doi:10.1016/0167-  
430 4889(87)90029-2 (1987).
- 431 30 Sprague, L. *et al.* Dendritic cells: in vitro culture in two-and three-dimensional collagen  
432 systems and expression of collagen receptors in tumors and atherosclerotic  
433 microenvironments. *Experimental cell research* **323**, 7-27 (2014).
- 434 31 Sadtler, K. *et al.* Design, clinical translation and immunological response of biomaterials  
435 in regenerative medicine. *Nature Reviews Materials* **1**, 1-17 (2016).
- 436 32 Mishra, P. K. *et al.* Sterile particle-induced inflammation is mediated by macrophages  
437 releasing IL-33 through a Bruton's tyrosine kinase-dependent pathway. *Nature materials*  
438 **18**, 289-297 (2019).
- 439 33 O'Neill, L. A. & Pearce, E. J. in *J Exp Med* Vol. 213 15-23 (2016).
- 440 34 Maitra, R., Clement, C. C., Crisi, G. M., Cobelli, N. & Santambrogio, L. Immunogenicity of  
441 modified alkane polymers is mediated through TLR1/2 activation. *PloS one* **3**, e2438  
442 (2008).
- 443 35 Tamaki, Y. *et al.* Increased expression of toll-like receptors in aseptic loose  
444 periprosthetic tissues and septic synovial membranes around total hip implants. *The*  
445 *Journal of rheumatology* **36**, 598-608 (2009).
- 446 36 Hodges, N. A., Sussman, E. M. & Stegemann, J. P. Aseptic and septic prosthetic joint  
447 loosening: Impact of biomaterial wear on immune cell function, inflammation, and  
448 infection. *Biomaterials* **278**, 121127 (2021).
- 449 37 Goodman, S. B., Pajarinen, J., Yao, Z. & Lin, T. Inflammation and bone repair: from  
450 particle disease to tissue regeneration. *Frontiers in Bioengineering and Biotechnology*,  
451 230 (2019).

- 452 38 Zhao, F., Cang, D., Zhang, J. & Zheng, L. Chemerin/ChemR23 signaling mediates the  
453 effects of ultra-high molecular weight polyethylene wear particles on the balance  
454 between osteoblast and osteoclast differentiation. *Annals of Translational Medicine* **9**  
455 (2021).
- 456 39 Koreny, T. *et al.* The role of fibroblasts and fibroblast-derived factors in periprosthetic  
457 osteolysis. *Arthritis & Rheumatism: Official Journal of the American College of*  
458 *Rheumatology* **54**, 3221-3232 (2006).
- 459 40 Man, K., Jiang, L.-H., Foster, R. & Yang, X. B. Immunological responses to total hip  
460 arthroplasty. *Journal of functional biomaterials* **8**, 33 (2017).
- 461 41 Dapunt, U., Prior, B., Kretzer, J. P., Giese, T. & Zhao, Y. Bacterial Biofilm Components  
462 Induce an Enhanced Inflammatory Response Against Metal Wear Particles. *Therapeutics*  
463 *and clinical risk management* **16**, 1203 (2020).
- 464 42 Xie, N. *et al.* Glycolytic reprogramming in myofibroblast differentiation and lung fibrosis.  
465 *American journal of respiratory and critical care medicine* **192**, 1462-1474 (2015).
- 466 43 Kisielinski, K., Cremerius, U., Reinartz, P. & Niethard, F. Fluorodeoxyglucose positron  
467 emission tomography detection of inflammatory reactions due to polyethylene wear in  
468 total hip arthroplasty. *The Journal of arthroplasty* **18**, 528-532 (2003).
- 469 44 Reinartz, P. *et al.* Radionuclide imaging of the painful hip arthroplasty: positron-emission  
470 tomography versus triple-phase bone scanning. *The Journal of Bone and Joint Surgery.*  
471 *British volume* **87**, 465-470 (2005).
- 472 45 Kuo, J., Foster, C. & Shelton, D. Particle disease on fluoride-18 (NaF) PET/CT imaging.  
473 *Journal of Radiology Case Reports* **5**, 24 (2011).
- 474 46 van der Bruggen, W., Bleeker-Rovers, C. P., Boerman, O. C., Gotthardt, M. & Oyen, W. J.  
475 in *Seminars in nuclear medicine*. 3-15 (Elsevier).
- 476 47 Udagawa, N. *et al.* Interleukin (IL)-6 induction of osteoclast differentiation depends on  
477 IL-6 receptors expressed on osteoblastic cells but not on osteoclast progenitors. *The*  
478 *Journal of experimental medicine* **182**, 1461-1468 (1995).
- 479 48 Raghu, H. *et al.* CCL2/CCR2, but not CCL5/CCR5, mediates monocyte recruitment,  
480 inflammation and cartilage destruction in osteoarthritis. *Annals of the rheumatic*  
481 *diseases* **76**, 914-922 (2017).
- 482 49 Loi, F. *et al.* Inflammation, fracture and bone repair. *Bone* **86**, 119-130 (2016).
- 483 50 Liu, J. *et al.* Macrophage polarization in periodontal ligament stem cells enhanced  
484 periodontal regeneration. *Stem cell research & therapy* **10**, 1-11 (2019).
- 485 51 Ma, C., Kuzma, M. L., Bai, X. & Yang, J. Biomaterial-based metabolic regulation in  
486 regenerative engineering. *Advanced Science* **6**, 1900819 (2019).
- 487 52 Saborano, R. *et al.* Metabolic reprogramming of macrophages exposed to silk, poly  
488 (lactic-co-glycolic acid), and silica nanoparticles. *Advanced Healthcare Materials* **6**,  
489 1601240 (2017).
- 490 53 Gonçalves, R. & Mosser, D. M. The isolation and characterization of murine  
491 macrophages. *Current protocols in immunology* **111**, 14.11. 11-14.11. 16 (2015).
- 492 54 Feoktistova, M., Geserick, P. & Leverkus, M. Crystal violet assay for determining viability  
493 of cultured cells. *Cold Spring Harbor Protocols* **2016**, pdb. prot087379 (2016).
- 494



495 **Acknowledgements.** Euthanized C57BL/6J mice were a gift from RR Neubig  
496 (facilitated by J Leipprandt) and the Campus Animal Resources at Michigan State  
497 University (MSU). Funding for this work was provided in part by the James and  
498 Kathleen Cornelius Endowment at MSU.

499  
500 **Author contributions.** Conceptualization, C.V.M. and C.H.C.; Methodology, C.V.M.,  
501 S.B.G., and C.H.C.; Investigation, C.V.M., M.O.B., M.M.K. and M.H.; Writing – Original  
502 Draft, C.V.M.; Writing – Review & Editing, C.V.M., M.O.B., M.M.K., M.H., S.B.G. and  
503 C.H.C.; Funding Acquisition, C.H.C.; Resources, S.B.G. and C.H.C.; Supervision, S.B.G.  
504 and C.H.C.

505  
506 **Competing interests.** The authors declare no competing interests.